Practical guidelines for reproducible N_2O flux chamber measurements in nutrient-poor ecosystems

Nathalie Ylenia Triches [1,2], Jan Engel [1], Abdullah Bolek [1], Timo Vesala [3], Maija E. Marushchak [4], Anna-Maria Virkkala [5], Martin Heimann [1], and Mathias Göckede [1]

[1]Department of Biogeochemical Signals, Max Planck Institute for Biogeochemistry, Jena, Germany
[2]Institute for Atmospheric and Earth System Research/Forest Sciences, Faculty of Agriculture and Forestry, University of Helsinki, Helsinki, Finland
[3]Institute for Atmospheric and Earth System Research/Physics, Faculty of Science, University of Helsinki, Helsinki, Finland
[4]Department of Environmental and Biological Sciences, Faculty of Science, Forestry and Technology, University of Eastern Finland, Kuopio, Finland
[5]Woodwell Climate Research Center, Falmouth, USA

Correspondence: Nathalie Ylenia Triches (ntriches@bgc-jena.mpg.de)

Abstract. The atmospheric concentration of nitrous oxide (N_2O) has increased significantly since 1800, mainly due to agricultural activities. However, due to their large area, nutrient-poor natural soils, including those in the (sub-) Arctic, also play a crucial role in N_2O emissions and consumption. Despite their importance, these soils have been understudied due to methodological limitations in detecting low fluxes. Our study addresses this knowledge gap by testing a fast-responding, portable gas analyser (PGA; Aeris MIRA Ultra N_2O/CO_2) combined with manual chambers (height and diameter: 25 cm) for measuring N_2O fluxes from a nutrient-poor, sub-Arctic peatland. Our results show that this setup can detect and quantify low N_2O flux rates, with a mean and standard error of $-0.61 \pm 0.08\,\mu g N_2O\text{-}N\,m^{-2}h^{-1}$ for a 5-min closure time, as observed in our study. More than 70% of the measured N_2O fluxes exceeded the minimum detectable flux ($0.027 \pm 0.0002, \mu mol\,m^{-2}h^{-1}$), which varied according to chamber closure time. Our study highlights the importance of using fast-responding analysers to measure low N_2O fluxes and improve our understanding of diverse N_2O flux dynamics. For nutrient-poor soils, we recommend a chamber closure time of approximately 5 minutes. We also found that a non-linear flux calculation model yielded better results and was broadly applicable, including cases where data were linearly distributed. Overall, our study demonstrates the potential of fast-responding analysers to improve our understanding of N_2O flux dynamics in nutrient-poor soils.

1 Introduction

Nitrous oxide (N_2O) is the third most important greenhouse gas (GHG) with a global warming potential almost 300 times stronger than carbon dioxide (CO_2) over a period of 100 years (IPCC, 2023). It stays in the atmosphere for around 110 years, and its atmospheric concentration has increased from 273 ppb to 336 ppb since 1800 (Thoning et al., 2022). As most of this increase can be attributed to human activities, particularly the use of nitrogen (N) fertilisers in agriculture, research has focused on N_2O emissions from managed, agricultural soils (De Klein et al., 2020) that hold the potential for high N_2O emissions.

This is because the input of N increases the readily available mineral N needed for plant growth and thus increases harvest, but, simultaneously, can also result in higher N_2O emissions (Myhre et al., 2013).

Until about 15 years ago, few studies investigated N_2O fluxes in the (sub-) Arctic, where soils often have a very low availability of reactive N (Virkkala et al., 2024) and thus are not expected to emit amounts of N_2O relevant for the global climate (Voigt et al., 2020; Christensen et al., 1999; Grogan et al., 2004; Martikainen et al., 1993). In these low N ecosystems, N_2O uptake could be expected, but has, so far, not been confirmed in field studies (Buchen et al., 2019; Schlesinger, 2013). Since 2009, multiple studies have reported N_2O emissions similar to agricultural soils from organic-rich ecosystems in the Arctic (Repo et al., 2009; Marushchak et al., 2011; Elberling et al., 2010), shifting the focus to only selected, high-nutrient areas within the (sub) Arctic. Nevertheless, reporting near-zero N_2O fluxes is crucial to avoid overestimating emissions caused by biased site selection favouring high-emitting areas (Voigt et al., 2020).

In most studies, N_2O concentrations were sampled repeatedly with a syringe from the head space of a closed flux chamber and measured with a gas chromatograph (GC) in the laboratory (Hensen et al., 2013; Denmead, 2008; Pavelka et al., 2018). With this approach, typically between 4 and 6 discrete air samples are taken to measure the trend in N_2O mixing ratios during chamber closure time and calculate the fluxes. The sensitivity of GCs varies, but with only few samples drawn from a fluctuating time series that may not necessarily display a linear trend, differences in low concentrations are hard to capture and highly dependent on single data points (Hübschmann, 2015). Additionally, in previous studies, opaque chambers have been mostly used because temperature inside the chamber would increase less above the ambient temperature compared to transparent chambers (Clough et al., 2020). As a result, there are only few studies investigating N_2O fluxes under different light conditions (Stewart et al., 2012). Since this was the only available method for *in situ* N_2O measurements in the field, our knowledge on (sub-) Arctic N_2O fluxes is rather limited and makes it challenging to establish accurate baseline estimates, which are essential for detecting changes in fluxes.

Recent advances in laser spectroscopy led to novel, portable (< 15 kg) and fast-responding (1 Hz, *i.e.,* sampling every second) GHG analysers, offering new possibilities to measure low N_2O concentrations in nutrient-poor ecosystems (Subke et al., 2021). These portable gas analysers (PGAs) allow near-continuous monitoring of concentration changes, providing higher precision and lower detection limits than GC-based methods (Hensen et al., 2013). While differences in flux estimates between PGAs and GCs have been well-documented for CH_4 and CO_2, few studies have focused on N_2O (Christiansen et al., 2015; Brümmer et al., 2017). The detection limit was a significant constraint, as many reported N_2O fluxes were below the threshold of the GC method, limiting the ability to accurately asses their magnitude and trends. The availability of PGAs for *in situ* N_2O flux measurements raises new methodological questions. Unlike CH_4 and CO_2, where, under a fixed chamber height, approximately 3 minutes are well-accepted for reliable measurement, the minimal chamber closure time for N_2O fluxes flux in nutrient-poor ecosystems is unclear. This is because N_2O concentrations are very low and take longer to accumulate in the head space to accurately detect trends (Fiedler et al., 2022). Few studies have investigated the chamber closure time with portable N_2O analysers, and the reported recommendations range between 3 and 10 min and originate from ecosystems with higher N_2O flux rates (Fiedler et al., 2022; Brümmer et al., 2017).

The chamber community has been discussing the use of linear (LM) or non-linear (HM) models to calculate flux rates for decades (Pumpanen et al., 2004). The critique on the linear models is that they underestimate the flux rates due to the assumption that GHG concentrations keep increasing within the chamber head space (Fiedler et al., 2022; Hüppi et al., 2018). However, it is clear from the theory of molecular diffusion that the rate of concentration change within the chamber declines over time (Hutchinson and Mosier, 1981; Kutzbach et al., 2007; Kroon et al., 2008). As a result, there have been great efforts to implement non-linear flux calculations as alternatives to LM, for example, through software packages (Pedersen et al., 2010; Hüppi et al., 2018). However, non-linear flux calculations are not commonly used in the chamber community, likely because they are more complex to implement. For N_2O, there is a lack of data sets from nutrient-poor ecosystems to evaluate the effect of LM and HM models.

The main aim of this paper is to present a mobile flux chamber method capable of quantifying (very) low N_2O fluxes in nutrient-poor ecosystems. Using a novel portable N_2O analyser (Aeris MIRA Ultra N_2O/CO_2) and our custom-made transparent and opaque flux chambers, we provide the first extensive data set of low N_2O fluxes from the (sub-) Arctic. We tested the performance of our PGA in the laboratory and in the field across various land cover types from a thawing permafrost peatland in sub-Arctic Sweden. We compared N_2O flux rates calculated from different chamber closure times (3 min- 10 min) and evaluated differences between linear and non-linear calculation methods. Additionally, we compared flux rates based on high-frequency *in situ* observations against an approach that randomly draws discrete data points from the full time series, mimicking a GC-based approach. Finally, we aim to provide guidance on measuring N_2O fluxes in nutrient-poor ecosystems, such as the Arctic. Ideally, this will encourage researchers to measure low fluxes in (sub-) Arctic regions, get a better process understanding of N_2O fluxes, and determine how the N cycle in nutrient-poor ecosystems will respond to Arctic warming.

2 Methods

To facilitate the reader's understanding, we use the terminology proposed by Fiedler et al. (2022), with location describing the area where sampling occurs ("Stordalen mire"), site describing a vegetation unit within the location ("palsa lichen", "palsa moss", "bog", "fen"), and chamber base position (*i.e.*, plot) for the exact spot where N_2O was measured. With "chamber closure time", we specify the time frame a chamber was closed onto the soil; one of these periods is then called "measurement period".

2.1 Study location and sampling sites

All data were collected at the Stordalen mire, a complex palsa mire underlain by sporadic permafrost located in subarctic Sweden (68° 20.0' N, 19° 30.0' E), 10 km east of Abisko (Ábeskovvu in Northern Sámi language). Permafrost has been rapidly thawing at this location over the last decades, and only remains in the dry uplifted areas on the peatland (palsas) (Sjögersten et al., 2023). For our study, we randomly selected 24 chamber base positions in three transects on a dry-to-wet thawing gradient from palsa to bog to fen, with 6 replicates for each land cover type: palsa lichen, palsa moss, bog, and fen (Fig. 1). Transects 1 and 2 each contain 6 chamber base positions and are located in the northern centre of the mire, within the

footprint of an Integrated Carbon Observation System (ICOS, SE-Sto) eddy covariance tower which has been operating since 2014 (Lundin et al., 2024), Fig. 1). Transect 3 lies in the most north-eastern part of the palsa.

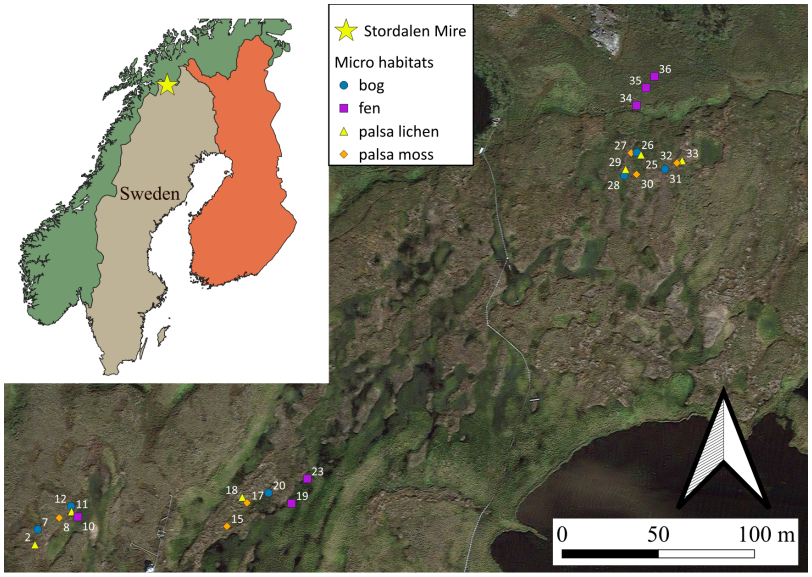

Figure 1. Three transects with chamber base positions in Stordalen overlaid on satellite image from ©Google Maps. The location of the Stordalen mire is marked with a star. Here, micro habitats are represented with different colours and symbols for clarity. The spatial data of each country can be found at https://simplemaps.com, last access: 17/09/2024)

Vegetation on the palsa is mainly dominated by lichen (*Cladonia spp.*), shrubs (*Empetrum hermaphroditum*, *Betula nana*, *Vaccinium uliginosum*, *Vaccinium vitis-idaea*, *Rubus chamaemorus*) and some mosses (*Dicranum elongatum*, *Sphagnum fuscum*). Both bogs and fens contain peat-forming mosses (*Sphagnum balticum*, *Sphagnum lindbergii*, *Sphagnum riparium*), with the dominant vascular plants on fens being cotton grass (*Eriophorum vaginatum*, *Eriophorum angustifolium*) and in bogs sedges (*Carex rotundata*, *Carex rostrata*). The soils in the area are classified as organic histosols or, if permafrost occurs within 2 m of cryoturbation activities, as cryosols (Siewert, 2018). Research at the Stordalen mire has been conducted for over a century (Jonasson et al., 2012; Callaghan et al., 2013), and a vast amount of data on CH_4 and CO_2 fluxes has been published (Łakomiec et al., 2021; Varner et al., 2022). The mean annual temperature at the Stordalen mire is -0.6°C and the annual precipitation 304 mm (Malmer et al., 2005).

The data presented in this study were collected during three separate campaigns covering different seasons: spring (between 23 - 30 May 2023), summer (20 - 27 July 2023), and autumn (3 - 22 September 2023). PVC collars with an inner diameter of 245.1 mm, a height of 150 mm, and a wall width of 4.9 mm were inserted into the soil on 29 August 2022. We inserted them as deeply as possible, between 100- 140 mm, to ensure a proper seal between the chamber head space and the atmosphere even during strong wind conditions, and in the palsa where the top peat was dry and highly porous. Between the collar and the chamber, we placed a custom-made sealing ring to avoid ambient air entering the chamber during our measurements (Fig.

2, S2). The sealing ring has an inner and outer diameter 235 and 265 mm, respectively, a height of 30 mm and is build from a metal ring wrapped in foam material (50 mm on each side). Tests confirmed that it sealed the chamber and the collar even under high wind conditions with up to 18 ms^{-1} wind gusts.

2.2 Chamber and portable gas analyser (PGA) setup and protocol

For our measurements, we used a custom-built static, non-steady state, non-flow-through chamber (Livingston and Hutchinson, 1995) made from acrylic glass (Göli GmbH) with a height of 250 mm and a diameter of 250 mm (Fig. 2, S1). We placed a fan (SUNON Maglev, 80 mm x 80 mm x 25 mm, 2000 RPM) inside the chamber to ensure well mixed conditions within the chamber during the measurements. Additionally, we installed a relative humidity (RH) and temperature probe (EE08, E+E Elektronik, Germany) and a pressure sensor (61402V, RM Young) for measuring essential parameters to calculate the fluxes. We equipped the chamber with quick-release connectors on top to connect the inlet and outlet tubing to the portable gas analysers. As complementary variables, we measured soil temperature at 15 cm (PT100 4-wire sensors, JUMO GmbH & Co. KG) at each quadrant outside of the plot, soil moisture at 12 cm and 30 cm (CS655-DS and CS650-DS, Campbell Scientific), and photosynthetically active radiation (PAR) (PQS1, Kipp and Zonen). More detailed information on our chamber setup can be found in the supplementary information.

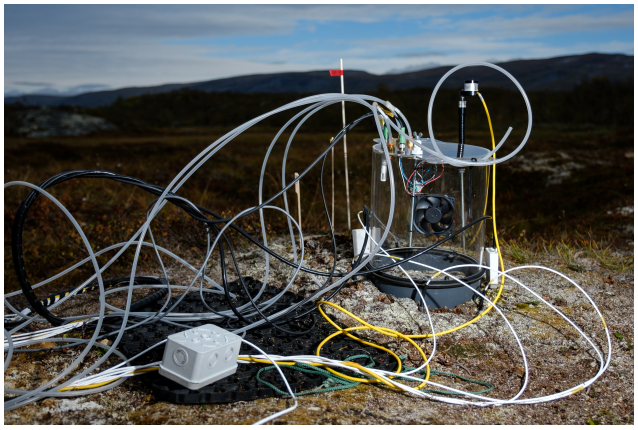

Figure 2. Chamber setup during measurement period, with soil moisture and soil temperature sensors installed in the soil, and all inlets connected. Photo: Fabio Cian, "Ubiquitous Anomaly", CC BY-NC-ND 4.0

To measure N_2O concentrations, we used the Aeris MIRA Ultra N_2O/CO_2 (from now onward: Aeris-N_2O) analyser (Aeris Technologies; sensitivity: 0.2 ppb/s for CO_2 and N_2O, frequency: 1 Hz). As most PGAs, the Aeris-N_2O provides dry mole fractions of the target gas. We performed several laboratory tests to assess the signal stability (*i.e.*, drifts and stabilisation time), uncertainties, noise level, and water interference of the Aeris-N_2O. Furthermore, we tested the impact of the humidity on the Aeris-N_2O analyser using a portable dew point generator (LI-610, Licor USA). By adjusting the dew point temperature, we examined four different humidity levels: 28, 45, 60, and 83 %. A calibration gas tank with a known N_2O concentration of

333.2 ppb was first connected to the dew point generator. The humidified gas was then connected to the Aeris-N_2O analyser inlet and each humidity level was sampled for about 20 minutes. Nevertheless, only a 10-minute window was used for further analysis due to relatively long time (about 10 min) required for the humidity levels to stabilise (see Fig. A2).

In the field, we attached a custom made external battery box with two $LiFePO_4$ batteries ($LiFePO_4$ 12.8V 20Ah, Green Cell) to the Aeris-N_2O, which could be switched whilst the analyser was running. In this study, one $LiFePO_4$ 12.8V 20Ah battery lasted for the whole day of field measurements (8h - max. 12h). A data logger (CR1000X, Campbell Scientific) was used to log all the sensor data including greenhouse gas concentrations which was placed inside a Pelican-case (Fig. S3 and S4). All GHGs and explanatory variables were logged with a frequency of 1 Hz. With this setup, all necessary information for the analyses was synchronised in a single data file, rather than many individual files from individual sensors and loggers.

Before we started a measurement period (*i. e.*, time when chamber is closed), we attached the tubes from the PGA to the chamber, ventilated the chamber for at least one minute, and gently closed it onto the sealing ring. The default chamber closure time for all measurement periods was 10 minutes. For dark measurements, a custom-made, light-impermeable tarp was placed over the chamber to prevent light from entering and minimise temperature fluctuations. We refer to these measurements as 'opaque' for clarity.

All data were processed in R (version 4.3.3; R Core Team, 2024) and version controlled in GitLab (the scripts are publicly available from https://git.bgc-jena.mpg.de/ntriches/data-analysis/-/tags/2024-12-12-triches-amtsubmission-n2oadvances). A filter script was applied to the data to ensure it met certain quality control standards, including:

- Removing data from the beginning of each measurement period to account for the time lag of gases moving through the tubes to reach the laser cell
- Removing implausible values (*e. g.,* -9999) of chamber pressure, chamber temperature, chamber relative humidity, soil temperature, volumetric water content, and PAR
- Replacing negative PAR values with 0
- averaging soil temperature readings gained from four sensors
- Detecting and removing flat lines indicating instrument failure (see SI 1.3)
- Pre-processing data for concentrations of N_2O, CO_2, and H_2O, as well as other relevant parameters.

2.3 Flux calculations

In our study, we calculated N_2Ofluxes using **all data points** from one measurement period. We removed 8 seconds in the start of the measurement period to account for the time delay until the concentration from the chamber reached the cell of the gas analyser. An extra 7 s were removed for opaque measurements, since we needed more time in the field to cover the chamber with the reflective tarp. To calculate the fluxes with both linear (LM) and non-linear (HM) methods in a reproducible way, we used the R package goFlux (v0.2.0, (Rheault et al., 2024)). We selected goFlux for several reasons: (i) it was specifically written

to process data gathered with PGAs, (ii) it uses measured temperature and pressure inside the chamber for flux calculation, (iii) it corrects for the dissolved gases in the water vapour inside the chamber, and (iv) it calculates fluxes using both LM and HM flux calculation methods. It also enables the comparison of results from LM and HM models using various statistical methods and flags, such as the minimal detectable flux (MDF, Eq. 4). Additionally, it generates plots for visualisation. For the flux calculation in LM, goFlux applies the commonly used linear equation as follows in Eq. 1:

$$F(t) = \frac{dC(t)}{dt}\frac{V}{A} \tag{1}$$

where $\mathrm{F(t)}$ is the gas flux rate at a given location during the chamber closure time (t), $\frac{dC(t)}{dt}$ is the mass concentration change with time, V is the volume of the chamber, and A the area of the soil covered by the collar (Subke et al., 2021). To report our flux rates, we used the atmospheric sign convention, *i. e.*, negative signs for an uptake of $\mathrm{N_2O}$ into the soil, and positive signs for emissions.

The HM model approach is based on the Hutchinson and Mosier (1981) approach as given in Eq. 2:

$$C(t) = \varphi + (C_0 - \varphi)e^{-\kappa t} \tag{2}$$

here, φ is the assumed constant gas concentration of the source within the soil (Pedersen et al., 2010), C_0 is the gas concentration in the chamber at the moment of chamber closure, and κ is the model parameter. To limit κ with a maximum threshold $\kappa_{\max}$, Eq. 3 was adapted from Hüppi et al. (2018).

$$\kappa_{\max} = \frac{F(t)}{\mathrm{MDF}\; t} \tag{3}$$

Here, the MDF is a theoretical threshold that represents the instrument's detection limit, based on its precision (η) provided by the manufacturer. However, it does not account for potential errors in the model or chamber artefacts, but reflects the instrument's inherent uncertainty. The MDF can be calculated using Eq. 4.

$$\mathrm{MDF} = \frac{\eta}{t}\,\theta \tag{4}$$

where, θ is a flux term that corrects for the water vapour inside the chamber and converts the flux unit to μmol $\mathrm{m^{-2}\ s^{-1}}$ and *t* is the measurement time, *i.e.*, the number of measurement points during the measurement period. This was calculated as given in Eq. 5

$$\theta = \frac{(1 - C_{\mathrm{H_2O}})V\,P}{A\,R\,T} \tag{5}$$

where C_{H_2O} is the water vapour concentration in mol mol^{-1}, P is the pressure inside the chamber in kPa, R is the universal gas constant in L kPa K^{-1} mol^{-1}, and T is the air temperature inside the chamber in K.

In the goFlux package, the fluxes that are below the detection limit are flagged. Note that owing to this function, all our flux estimates have their own MDF value. The package further implements the so called g-factor (g_f) (Hüppi et al., 2018) to restrict large curvatures of the non-linear flux models as follows (Eq. 6):

$$g_f = \frac{HM_F}{LM_F} \tag{6}$$

Here, HM_F and LM_F are the flux values that are calculated by HM and LM models, respectively. In this study, we used a g_f of 4, meaning that the flux calculated by the HM model can be max. 4 times higher than the flux calculated by the LM to avoid a large overestimation of fluxes (Eq. 6). We used this factor because, upon visual assessment, it fit our data best, and has been previously used (Leiber-Sauheitl et al., 2014). We did not use the mean absolute error nor the root mean square error to define if the HM or LM model performed better, since they were very similar among all measurement periods. We did also not use R^2 as a filter criteria since low and non-linear fluxes inherently results in low R^2 values (Kutzbach et al., 2007).

2.4 Data processing and simulations

We used our openly available script to simulate differences between chamber closure times and GC sampling, and the associated sensitivity analysis. We first calculated all fluxes using the original 10-minute chamber closure time (prec = 0.2, g.limit = 4). To see how different closure times affect N_2O fluxes, we shortened the closure time by 1 minute at a time, starting from 9 minutes, and recalculated the fluxes for each new time (*e.g.*, 9 minutes = 540 seconds, 8 minutes = 480 seconds, etc.). We compared how chamber closure time affects flux rates during transparent and opaque measurements, and identified the number of fluxes above the minimum detectable flux based on the goFlux output. While calculating our fluxes, we became aware of one chamber base position acting as a hot spot, *i. e.*, showing much higher flux rates than the other chamber base positions. Since we wanted to focus our analyses on low fluxes, we removed this hot spot from all analyses.

The simulations of GC measurements are based on drawing discrete sub-samples from the continuous *in situ* time series from the PGA, mimicking a sampling scheme where information on the increase of gas concentrations during chamber closure time is limited to a few snapshots in time. We simulated four scenarios: 3 GC samples (taken at 5 min, 7 min, and 10 min), 4 GC samples (3 min, 5 min, 7 min, and 10 min), 5 GC samples (1 min, 3 min, 5 min, 7 min, and 10 min), and 6 GC samples (1 min, 3 min, 5 min, 7 min, 8 min, and 10 min). For simulating the GC concentration, we picked the time stamp as defined above and took the average of 10 sec of N_2O concentrations measured by our PGA, *i. e.*, 5 seconds before and after the defined time stamp, as single GC point measurement (Fig. 9). We then calculated the resulting fluxes with goFlux (prec = 1.9, g.limit = 4) using a precision of 1.9 ppb according to sensitivity tests on an instrument at our laboratory (Agilent Technologies, 7890 B GC System, mean N_2O concentration 395.746 ppb with a SD of 1.875 ppb over ten repetitions), before we plotted the simulated versus original flux concentration measurements. To evaluate the performance of each sampling scheme, we compared the slopes, p-values, and R^2 values between the simulated and original data. To get an estimate on the uncertainties associated

with this GC simulation, we conducted a sensitivity analysis, where we did 21 simulations with a randomised selection of the 4 min sampling time (4 samples at 3,5,7,9 min), allowing a window of 60 sec around each selected GC point.

3 Results and discussion

3.1 Laboratory tests with the Aeris-N_2O

From the 15-hour ambient air sampling in our closed laboratory, we observed that the water vapour concentration in the ambient air dropped from approximately 2500 ppm to about 800 ppm within the first 30 min. It continued to decrease progressively throughout the sampling period; however, after 5 hours, the water vapour concentration somewhat stabilised, with a mean H_2O concentration of 476.9 ppm with a standard deviation of 18.7 ppm for the rest of the sampling. Note that these observed changes in water vapour might be partly due to the analysers warm-up period. We therefore discarded the initial 5 hours of data and used the remaining data to assess the signal stability and noise characteristics of the Aeris-N_2O. The Aeris-N_2O demonstrated a very stable signal with no apparent drift for about 10 hours of sampling period, having a low standard deviation of 0.290 ppb. Using Allan deviation plots (Allan, 1987), we evaluated the analyser's noise characteristics and found that the Aeris-N_2O showed low instrument noise, approximately 0.18 ppb at 2-second averaging (see Fig. 3).

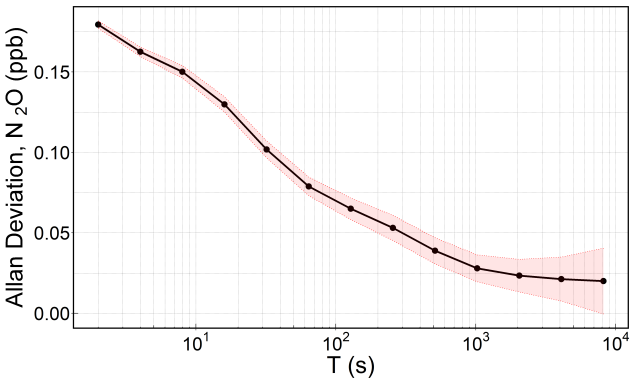

Figure 3. Computed Allan deviation plot based on 10 hours of continuous sampling, following a 5-hr spin up period during which the water vapour mole fraction was not stable. Here, T is the sampling time in log-scale and shaded region represents the 95% confidence interval.

Because PGAs are known to be sensitive to fluctuations in water vapour concentrations, we tested the Aeris-N_2O against different relative humidity (RH) conditions. Our tests with the four RH values (approx. 28%, 45%, 60% and 83%, respectively) showed that the water interference of the Aeris-N_2O was very small; we observed only slight differences in the mean N_2O concentrations for each humidity level (see Fig. 4), with mean N_2O concentrations of 332.7 ppb, 332.6 ppb, 332.7 pbb, and 332.5 ppb for RH values of 28%, 45%, 60%, and 83%, respectively. Furthermore, we observed the same standard deviation of about 0.3 ppb for each humidity level. Overall, our conducted laboratory tests indicated that the Aeris-N_2O was a suitable instrument for measuring low N_2O fluxes, showing low noise and water interference, along with negligible signal drift after

the laser warms up. Nevertheless, the long warm-up period (approximately 5 h) of the analyser needs to be taken into account, as this can be a limiting factor for certain applications. To mitigate this, the Aeris-N_2O remained powered on throughout the whole field campaign.

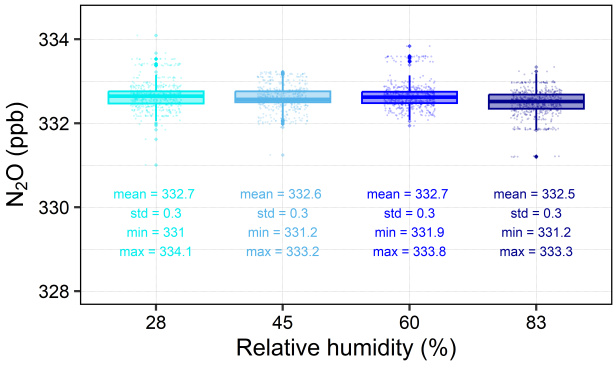

Figure 4. Measured N_2O concentrations for different relative humidity (RH) values, with basic statistics of each RH values summarised under each box plots. Each humidity level was sampled for approximately 20-mins; however, only a 10-min window was used for further calculations. For our tests, we used a standard gas with a mean of 333.16 $\pm$ 0.16 ppb as input. Jittered points are overlaid on the boxplots to visually separate overlapping data points, illustrating the distribution and density of the data.

3.2 Impact of chamber closure time on N_2O fluxes

At our site, we commonly observed net N_2O consumption, suggesting an atmospheric sink, with a mean flux of -0.469 μg N_2O-N $m^{-2} h^{-1}$ and a 95% confidence interval (CI) of (-0.60,-0.3) during a chamber closure time of 10 min. Our calculated mean flux during transparent measurements was 0.361 μg N_2O-N $m^{-2} h^{-1}$, with a 95% CI of (0.24,0.48) during a chamber closure time of 10 min (Table 1). For opaque measurements, our calculated flux was -1.29 μg N_2O-N $m^{-2} h^{-1}$, with a 95% CI of (-1.45,-1.13), indicating that our opaque measurements represent a real biochemical process, rather than an experimental artefact, in the (sub-) Arctic ecosystem. Nevertheless, the impact of environmental drivers on N_2O fluxes, including the transparent and opaque measurements, is beyond the scope of this study. Overall, we collected 338 samples, with 60-90 % of N_2O fluxes above the detectable limit. We therefore also acknowledge the possibility of unknown chamber artefacts that may remain undiscovered and could affect the interpretation of our data.

While chamber measurements are essential for understanding GHG emissions, they can alter soil-air conditions and introduce observational artefacts. These include potential impacts such as pushing atmospheric air into the soil when closing the chamber, flushing soil gas into the chamber head space, and changing conditions during closure, *e.g.*, increasing temperature and humidity inside the chamber due to soil and plant evaporation (Subke et al., 2021; Rochette and Eriksen-Hamel, 2008). As a result, the N_2O concentration gradient between the soil and the chamber head space and potentially also the functioning of plants and soil microbes are altered and may cause a bias in the flux estimates (Davidson et al., 2002). At our site, condensation within the chamber during a measurement period increased drastically with time, especially in the colder months. Although

Table 1. Comparison of chamber closure times for both transparent and opaque measurements, with SE = Standard Error, CI = confidence interval, and % = percentage difference between the absolute mean flux of chamber closure time x compared to chamber closure time 10 min. CI is the margin of error calculated at 1.96 * SE; the lower CI is calculated as mean flux - CI, the upper CI as mean flux + CI.

Chamber closure time	Transparent / opaque	Mean flux	SD flux	n	SE	CI	lower CI	upper CI	%
3	light	-0.00	1.54	169	0.12	0.23	-0.24	0.23	98.97
3	dark	-1.49	1.80	170	0.14	0.27	-1.76	-1.22	-15.16
4	light	0.20	1.26	169	0.10	0.19	0.01	0.39	43.58
4	dark	-1.51	1.53	170	0.12	0.23	-1.74	-1.28	-16.92
5	light	0.26	1.06	169	0.08	0.16	0.10	0.42	27.52
5	dark	-1.47	1.39	170	0.11	0.21	-1.68	-1.26	-14.18
6	light	0.30	0.94	169	0.07	0.14	0.16	0.45	16.21
6	dark	-1.43	1.29	170	0.10	0.19	-1.62	-1.24	-10.75
7	light	0.33	0.89	168	0.07	0.14	0.19	0.46	9.41
7	dark	-1.39	1.24	170	0.10	0.19	-1.58	-1.21	-8.05
8	light	0.35	0.83	168	0.06	0.13	0.23	0.48	2.35
8	dark	-1.35	1.21	170	0.09	0.18	-1.54	-1.17	-4.92
9	light	0.36	0.81	168	0.06	0.12	0.24	0.48	1.00
9	dark	-1.34	1.16	170	0.09	0.17	-1.51	-1.17	-3.79
10	light	0.36	0.80	168	0.06	0.12	0.24	0.48	0.00
10	dark	-1.29	1.07	170	0.08	0.16	-1.45	-1.13	0.00

our laboratory tests showed that for the Aeris-N_2O, increased water vapour does not interfere with N_2O concentrations, all laser cells are sensitive to water vapour. Too high water vapour contents can, even with a filter assembly (1 micrometers pore size) within the tube, reach the analyser cell and lead to an abrupt end of a field campaign (Fiedler et al., 2022). It is, therefore, crucial to know how water vapour concentrations vary over time during chamber closure. At our study site, H_2O concentrations during transparent measurements increased, on average, from below 10000 ppm up to >16000 ppm, depending on the season. When we look at the rate of change over each minute, *i.e.*, 0-1 min, 1-2 min, 2-3 min etc., we can see that this rate of change drastically decreased within the first 2 min, and then exponentially decreased with increasing chamber closure time (Fig. S5). In other words, H_2O concentrations rose drastically in the first 2 min (> 1300 ppm; data not shown), after which they levelled out until around 8 min, before they started increasing again (Fig. S5). For opaque measurements, the impact followed the same pattern, but was of much smaller magnitude (approx. 600 ppm rise within the first 2 min; data not shown). Because the increase of H_2O concentrations did not directly affect N_2O concentrations in our study, and was further considered when calculating the fluxes with goFlux (Rheault et al., 2024), we did not introduce further measures.

When using transparent chambers, temperature control is an additional constraint (Rochette and Hutchinson, 2015). Ideally, the chamber temperature remains stable throughout the measurement period. However, in the field, especially during sunny conditions, this is challenging to achieve without active cooling, as the chamber's transparency creates a greenhouse effect

(Rochette and Hutchinson, 2015). An increase in temperature can enhance microbial activity, leading to either N_2O production or consumption and potentially causing biased N_2O concentrations (Rochette and Eriksen-Hamel, 2008; Clough et al., 2020). In our study, chamber temperatures during transparent measurements changed similarly to H_2O concentrations, with the strongest decrease occurring within the first minutes of the measurement period (Fig. S5 and S6). At our site, temperature increased by around 0.7°C within the first two minutes, which slowed down to 0.3°C after 5 min (data not shown). During opaque measurements, temperature within the chamber decreased slightly by max. 0.2°C in the first two minutes, and below 0.1°C after three minutes (data not shown). It is likely that during transparent measurements, the abrupt temperature increase in the first two minutes may have impacted N_2O concentrations (Parkin and Venterea, 2010). However, we refrained from using cooling systems such as heat exchangers or ice packs since they also have drawbacks, *e.g.*, causing additional condensation within the chamber (Clough et al., 2020; Fiedler et al., 2022). As a result, we cannot exclude potential temperature effects on our N_2O concentrations during our measurement periods. Even though temperature changes are considered in the final flux calculation (Rheault et al., 2024), we argue that temperature changes inside chambers call for shorter closure times.

To minimise disturbances to the soil gas-atmosphere gradient and obtain flux estimates close to pre-deployment levels, several researchers have recommended using short chamber closure times of around 5 minutes (Fiedler et al., 2022; Pavelka et al., 2018; Venterea and Baker, 2008). This is because during chamber closure, mean flux rates vary as N_2O builds up or decreases in the chamber head space (Rochette and Hutchinson, 2015). As closure time increases, the concentration gradient between soil and chamber head space decreases, reducing the diffusive flux. Within a closed system, gases can reach a temporary state of equilibrium over time, where the rate of N_2O production in the soil balances with the rate of N_2O release into the chamber head space(Fiedler et al., 2022). Our results suggest that for transparent measurements, a chamber closure time of 3 min is too short and may result in significantly lower flux rates than longer chamber closure times (ANOVA, $p < 0.05$ for 3 min compared to 8, 9, and 10 min; Fig. 5). This discrepancy may be attributed to low microbial activity, or the possibility that N_2O production is countered by its rapid uptake or dissolution in the water present in the soil matrix, a phenomenon previously observed for CO_2 (Widén and Lindroth, 2003). From 4 min onward, our calculated mean N_2O flux rates are not significantly different from one another (Table 1). The proportion of transparent fluxes above the minimum detectable flux (MDF) increased from 62.7% to 78.6 % as closure time increased from 3 to 10 minutes (Fig. 5 a)). While longer closure times reduce uncertainty and the amount of fluxes below the MDF, the gain is small after 4 minutes. We thus recommend chamber closure times of more than 4 minutes for reliable N_2O flux estimates, as this balances the need for accurate transparent measurements while minimising soil disturbance, as well as the impact of increasing temperature on N_2O concentrations within the chamber.

For opaque measurements, we find that our calculated fluxes show higher N_2O uptake from shorter chamber closure times, with flux rates around 15% lower at 3 - 5 min than at 10 min, respectively (Table 1). At 6 min, the differences in our calculated N_2O uptake was still 10% higher than at 10 min, decreasing to below 8% between 7 and 9 min. At the same time, the MDF increased from 56.5% to 87.1% between 3 min and 10 min (Fig. 5 b)). Nevertheless, none of the flux rates across different closure times were significantly different from one another (Kruskal-Wallis, $p = 0.99$). Especially for N_2O uptake, it is essential to keep the chamber closure time as short as possible. This is because N_2O availability through soil diffusion is often the limiting factor for microbial consumption, *i.e.*, atmospheric N_2O consumption by N_2O-reducing microbes (Liu

et al., 2022). When the chamber is closed, the N_2O concentration in the head space decreases as it diffuses into the soil, driven by the concentration gradient. As a result, the uptake rate also decreases, since N_2O reduction may become substrate limited. Consequently, long chamber closure times may underestimate the uptake of atmospheric N_2O. Our analysis of the chamber closure time confirms this: during opaque measurement, we found that the uptake rate at 3-5 minutes were greatest, and decreased with every minute of added chamber closure time (Fig. 5). For opaque measurements, we therefore suggest to keep the chamber closure time between 3-5 min, unless very few data points are available, when aiming for fluxes above the MDF becomes more important.

With the goFlux output, we obtain an individual MDF for each measurement period, allowing us to determine on a case-by-case basis if a flux is above the MDF. For both transparent and opaque measurements, the MDF in our study was, on average, $0.03\,\mu$mol $m^{-2}h^{-1}$. This is lower than the reported $0.18\ \mu$mol $m^{-2}h^{-1}$ MDF rates in other nutrient-poor ecosystems by Christiansen et al. (2015) (Table 1). However, as mentioned above, more than 40% of the fluxes were below the MDF at 3-minute closure time. This confirms that very short closure times can lead to higher uncertainties of flux estimates because the concentration changes are too small to be accurately detected (Fiedler et al., 2022). It is, therefore, essential to consider the precision of the instruments used in the field to identify the best-suited chamber closure time. With the Aeris-N_2O, we recommend chamber closure times above 4 min for transparent N_2O measurements in low nutrient ecosystems. The optimal closure time depends on factors such as effective chamber height, micro habitat, and the duration of the field campaign. Shorter closure times allow for more repetitions, increasing the number of observation per chamber base position or adding more replicates, which is essential for the accurate representation of spatial variability (Jungkunst et al., 2018). For opaque measurements, we suggest shorter chamber closure times of 3-5 min. These findings are in line with other studies (Cowan et al., 2014; Kroon et al., 2008; Christiansen et al., 2015) but confirm, for the first time, that these recommendations are applicable to (very) nutrient-poor ecosystems.

3.3 Impact of linear and non-linear flux calculation approaches on N_2O fluxes

To facilitate understanding of how N_2O concentration build-up or reduction in the chamber head space can result in different flux estimates, goFlux automatically produces scatter plots with defined criteria (Fig. 6). These outputs allow for visual control of all measurement periods; additionally, csv outputs with the pre-defined quality checks are automatically produced. Our analysis using the goFlux package (Rheault et al., 2024) revealed that 59% (n = 2560) of all N_2O fluxes during different chamber closure times were best described by the HM model, indicating non-linear concentration changes over time. In contrast, 41% (n = 1728) of the fluxes were better explained by the LM model, showing a linear concentration change over time. However, all of the 41% fluxes calculated with the LM model had no HM flux, meaning that the software did not calculate a non-linear flux because the HM model gave the same results as the LM model, and therefore favoured the LM model. In other words, all fluxes were either calculated using the HM model or resulted in the same values as the LM model. This has two possible reasons: the first is that the linearity might be an outcome of short measurement time and low flux, so that the non-linear model was reduced to a linear model; the second is an overestimation of the flux (Kutzbach et al., 2007). Linear and non-linear models for concentration data during chamber closure may typically be seen as alternatives, not complementary approaches. However,

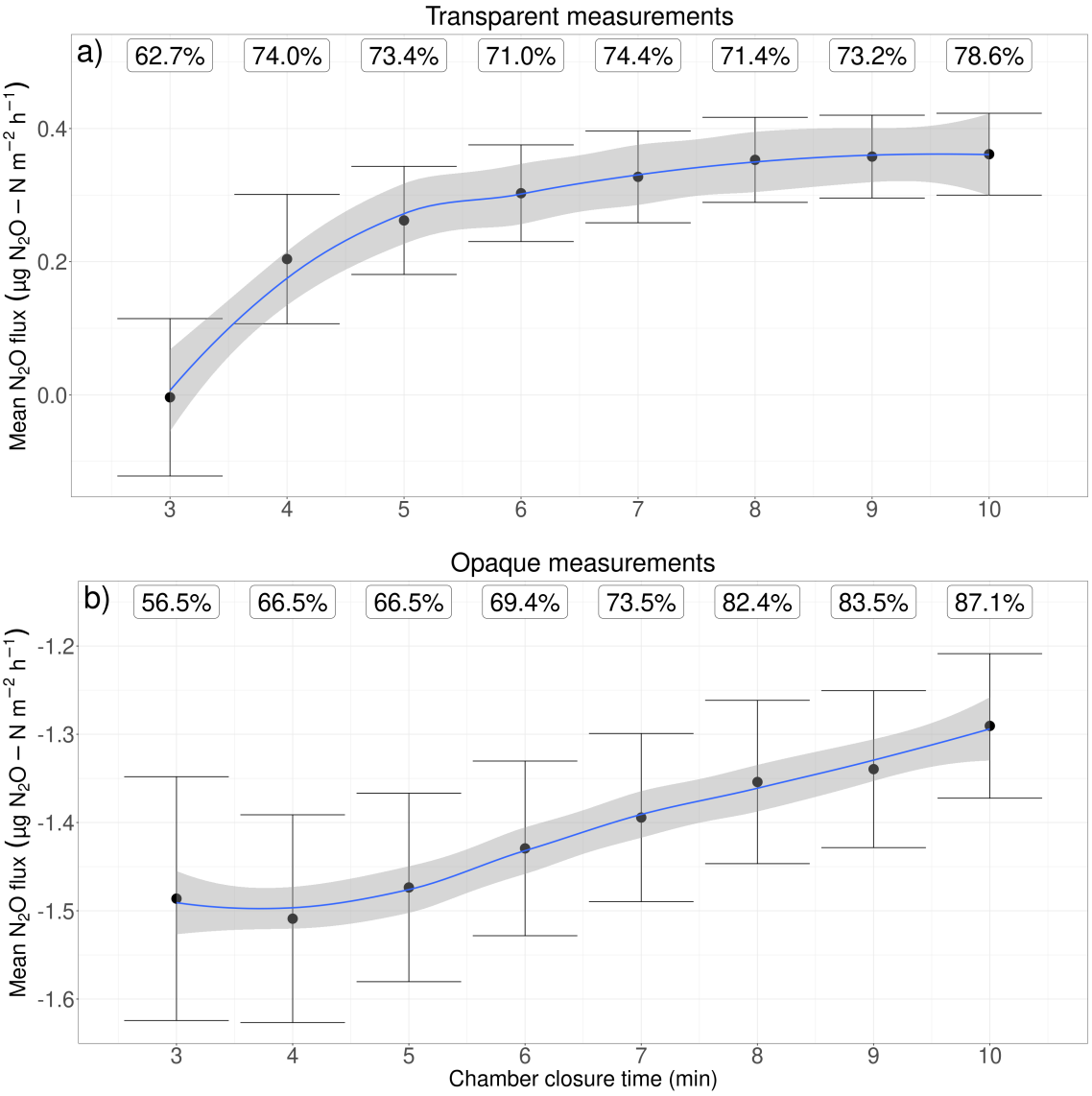

Figure 5. Mean N_2O *fluxes* (note: not concentrations) for transparent and opaque measurements, with number of measurement periods above the minimal detectable flux (MDF, %). Note the different y-axes for the upper and lower plots. The range indicates the upper and lower limit of the 95% confidence interval.

the non-linear fitting includes the linear fitting as a special case. When using a generic exponential function ae^{-bt} to fit data, where a and b are positive constants to be fitted, it can be approximated to a linear function if the data points are distributed linearly. This is because the exponential function can be expanded as a series, and when the rate constant b is small, the linear function dominates. Namely, the first three terms of the serial expansion are $a(1 - bt + (bt)^2/2$, but when b is very small, *i.e.,* $b << 1$, it is reduced to $a(1-bt)$, which is the linear form. The slope of the linear term is $-ab$; if we take the time derivative of the original exponential function to calculate the slope, it gives$-abe^{-bt}$. When we expand it as a series and only take the first order term as $b << 1$, we again obtain the simplified $-ab$ as slope. This means that if the data points are linear, the exponential fitting will automatically reduce to a linear fitting with the same slope. With our results, we show that for N_2O fluxes, indeed, flux estimates were reduced to the linear model and yielded identical results as the non-linear model. The second reason for favouring linear models in goFlux is that an unexplained nonlinearity can occur in curvature, *i.e.*, non-exponential curvatures, which can result in an overestimation of the flux estimates (Kutzbach et al., 2007). In goFlux, the curvature of the non-linear model can be restricted with g_f (see section 2.3). If the curvature was too large, leading to flux estimates over four times higher (with a g_f = 4) than those from the linear model, the linear model was favoured. When we used a lower g_f of 1.25 for comparison, *i.e.*, allowing HM fluxes to be max. 25% higher than LM, we found that about one-quarter of the fluxes estimated by the non-linear model would have been excluded due to significant overestimation.

There is a tendency to favour LM over HM models in literature, primarily due to their simplicity. It is also generally assumed that concentration changes are linear during short chamber closure times, keeping uncertainties low (Hüppi et al., 2018; Kroon et al., 2008). However, because GHG concentrations naturally follow a non-linear behaviour within a closed system due to diffusion theory (Fick's first law) and leakage (Anthony et al., 1995; Kroon et al., 2008), LM models may introduce a bias, differing from HM model estimates by up to 60% (Hüppi et al., 2018; Kroon et al., 2008), resulting in less accurate flux estimates and GHG budgets. This has been thoroughly investigated for N_2O fluxes by Kroon et al. (2008), who found a large underestimation of N_2O fluxes by the LM model in their study. With our results, we suggest that all future N_2O flux chamber calculations should be done using HM models, which can be filtered for overestimation of fluxes when flux rates are larger. Novel software packages such as goFlux (Rheault et al., 2024) offer the possibility to easily integrate both LM and HM models, and report the flux rates in a reproducible way. We believe that these approaches will be crucial to facilitate the use of both LM and HM models, and, as a consequence, enable the chamber community to standardise their flux calculation methods. We further emphasise the importance of using all available data points for flux estimates, rather than selecting a subset of linear data. This is because our approach, which involves filtering out unrealistic values and visually verifying measurement periods after flux calculation, enhances the reproducibility and consistency of N_2O flux estimates.

3.4 Simulated differences in N_2O flux rates between GC and PGA

Our results indicate that for transparent measurements, the N_2O fluxes we calculated using three simulated GC samples were, on average, 21.7% lower than the PGA fluxes (0.085 μg N_2O-N m^{-2},h^{-1}; data not shown). Specifically, positive values, *i.e.*, efflux, were generally underestimated ($p < 0.001$, $R^2_{adj} = 0.37$, Fig. 7). When we calculated fluxes using four simulated GC samples, negative N_2O fluxes appeared to be nearly identical with the N_2O uptake we calculated from the PGA (600 data

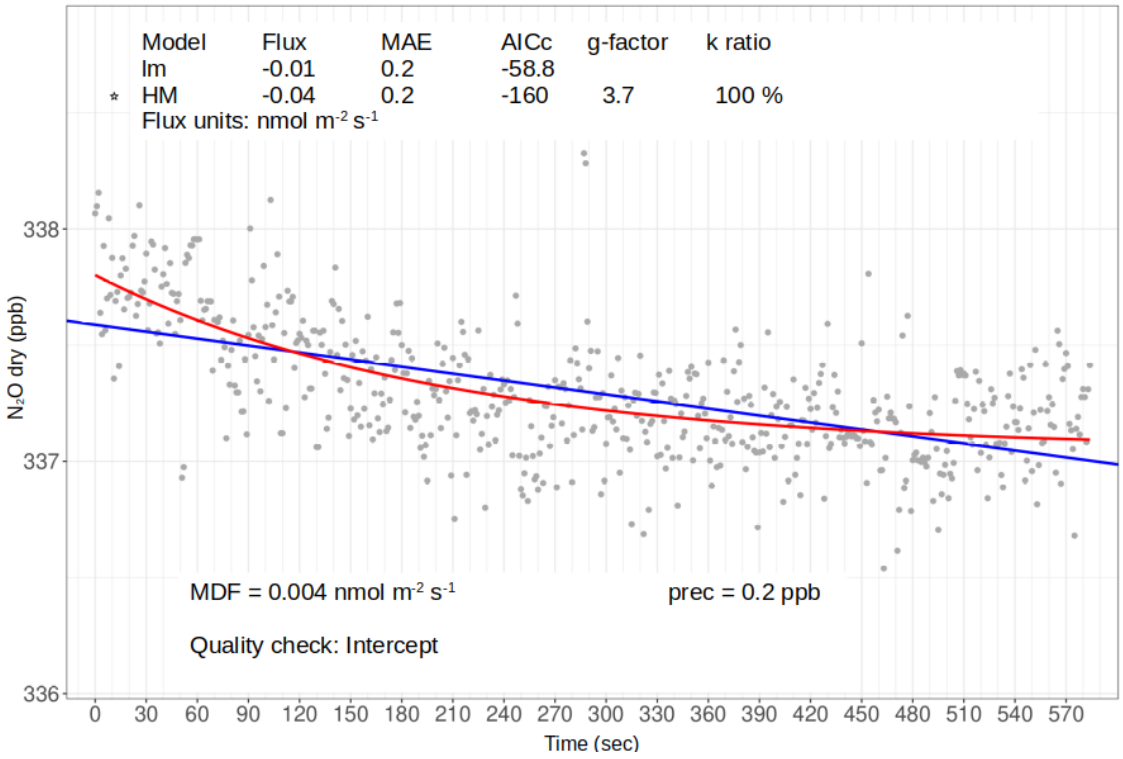

Figure 6. Example of scatterplot output from goFlux, showing N_2O concentrations in ppb from one measurement period, with information on linear (LM, blue line) and non-linear (HM, red line) flux calculations. For every measurement period, the chosen model is marked with a star (here, HM) according to the pre-defined quality check, indicated on the bottom of the graph (here, intercept). Flux values, mean absolute error (MAE), g-factor and k ratio are shown on top of the figure; here, a g-factor of 3.7 indicates that the HM flux value is 3.7 times higher than the one obtained from LM. Source: goFlux package (Rheault et al., 2024), font sizes modified.

points); however, efflux was still underestimated by 3% ($p < 0.001$, $R^2_{adj} = 0.65$). Interestingly, by increasing the sample size to five or six, our calculated fluxes seemed to underestimate N_2O uptake, whilst efflux was overestimated ($p < 0.001$, $R^2_{adj} = 0.85$, Fig. 7). Overall, the N_2O fluxes we calculated using five samples underestimated N_2O fluxes by 2.2%, while calculations with six samples resulted in an overestimation of around 2.4% (data not shown).

For opaque measurements, all N_2O flux estimates we calculated from GC simulations were lower than the fluxes estimates we calculated from the PGA, with an underestimation of 6.6%, 2.3%, 7.9%, and 8.1% for three, four, five, and six sample points (data not shown). With three samples, the calculated uptake rates were generally overestimated, while efflux was underestimated. When we calculated fluxes using four simulated GC- samples, N_2O uptake was still overestimated, while with five and six sample points, it was slightly underestimated. However, compared to transparent measurements, the R^2_{adj} values were low (Fig. 8, $R^2_{adj} = 0.21$, 0.51, 0.69, and 0.68, respectively). The underestimation of GC fluxes may occur as a result of a smoothed out curve: when only few data points are available, variations in curves are naturally reduced. Furthermore, the

precision of our GC was 1.9 ppb compared to 0.2 ppb of the Aeris-N_2O, resulting in less accurate measurements of the N_2O concentrations. This may lead to a loss of detail in the curve, particularly in the peak values of the N_2O concentrations, which can result in underestimation of the flux.

It is important to note that our comparison was made between our PGA and simulated GC measurements (Figure 9). For the GC simulations, we adjusted the instrument precision during the flux calculation, but no actual air samples were analysed by any GC instrument. Furthermore, our chamber closure time was considerably shorter than for most GC studies because of the condensation and temperature changes within the chamber. During prolonged chamber closure times, significant changes in the concentration gradient and chamber conditions can take place (see above), which are unlikely to be replicated in our GC-simulation. This difference in experimental design may actually be beneficial, as it allows us to isolate and study the effects of shorter closure times on N_2O flux measurements. Furthermore, our sensitivity analysis with 4 simulated GC samples showed that even when we changed the sample times $\pm$ 60 sec compared to the original time stamp, flux rates differed less than 10%, with R^2_{adj} values between 92 and 98 (data not shown). We believe that the underestimation of N_2O flux rates we calculated is, therefore, not a result of a inadequate simulation, but needs to be verified by future studies actually measuring N_2O samples from nutrient-poor ecosystems in a GC.

Our results are consistent with previous studies that compared N_2O flux rates between GCs and PGAs (Fig. 9), which concluded that GCs were suitable for measuring N_2O fluxes under certain conditions (Christiansen et al., 2015; Brümmer et al., 2017). Christiansen et al. (2015) investigated the differences between a fast-responding analyser (a cavity ring-down spectroscopy analyser (Fleck et al., 2013)) and a high-precision GC in agricultural fields in Vancouver (Canada) by taking five GC samples at 0, 3, 10, 20, and 30 min chamber closure time. They found that N_2O fluxes were very similar and did not differ significantly, with average N_2O fluxes of 47.6 $\pm$ 8.4 μg N_2O-N $m^{-2}h^{-1}$ from the the fast-responding analyser and 61.6 $\pm$ 11.2 μg N_2O-N $m^{-2}h^{-1}$ from GC, respectively. With a similar setup, Brümmer et al. (2017) compared N_2O fluxes measured by a fast-responding analyser similar to the Aeris-N_2O (a quantum cascade laser) and a GC from an low-flux agricultural grassland in Braunschweig (Germany). Their four GC samples taken at 0, 20, 40, and 60 min were highly scattered and rarely showed a distinctive trend, introducing a wide range of N_2O fluxes between -26 to 39 μg N_2O-N $m^{-2}h^{-1}$ with a standard error between 1 and 44 μg N_2O-N $m^{-2}h^{-1}$. In contrast, the N_2O fluxes measured by the fast-responding analyser only varied between 4 and 32 μg N_2O-N $m^{-2}h^{-1}$, with standard errors below 1.2 μg N_2O-N $m^{-2}h^{-1}$. This highlights three critical aspects: first, despite claiming low-flux environments, flux rates from agricultural fields are much higher than from a sub-Arctic peatland or other nutrient-poor ecosystems (Savage et al., 2014; Cowan et al., 2014), where capturing N_2O fluxes is even more challenging. Second, low N_2O fluxes tend to be very scattered, with large noise in comparison to the actual trend, *i.e.*, the change in concentration during chamber closure. This makes it very challenging to find trends when calculating fluxes if only few samples are available, let alone showing N_2O uptake without high uncertainties (Cowan et al., 2014). Finally, it is crucial to know and test the precision of the instruments used in the field to get reliable flux estimates and minimal detectable fluxes (Kutzbach et al., 2007; Christiansen et al., 2015).

Our findings suggest that calculating N_2O fluxes from three GC samples is likely to lead to an underestimation of the "real" flux (Kutzbach et al., 2007). We therefore strongly advise against using only three samples, as flux calculations may have to

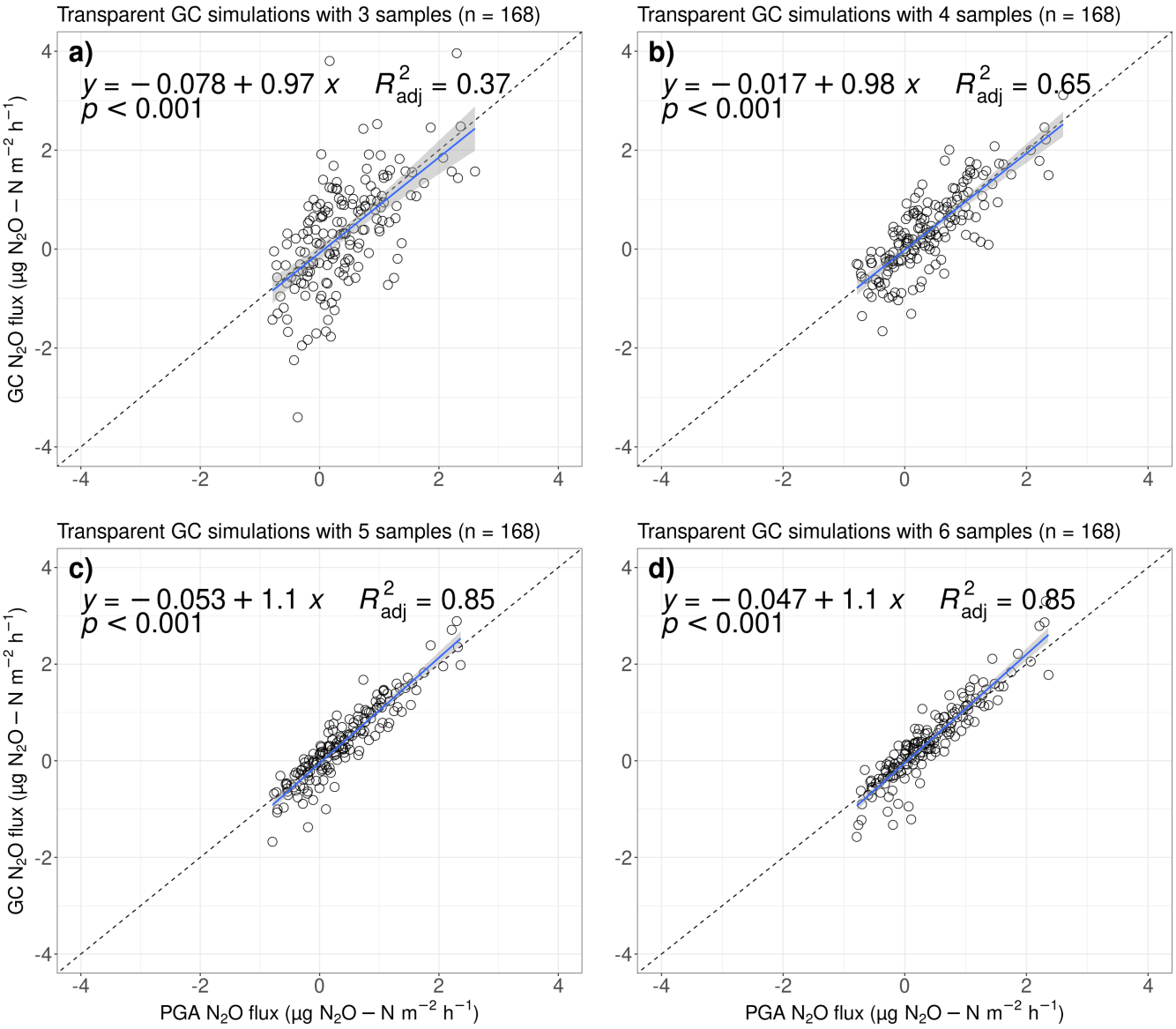

Figure 7. Simulated GC fluxes from light measurements with a) 3, b) 4, c) 5, and d) 6 samples compared to flux measurements taken with our PGA for 10 min (n = 168). All fluxes were calculated with the goFlux package; results from "best.Flux" are shown. The blue trend line fits a generalised linear model, with the shaded area representing the 95% confidence interval. The shown equations and R^2_{adj} values follow the $y \sim x$ equation.

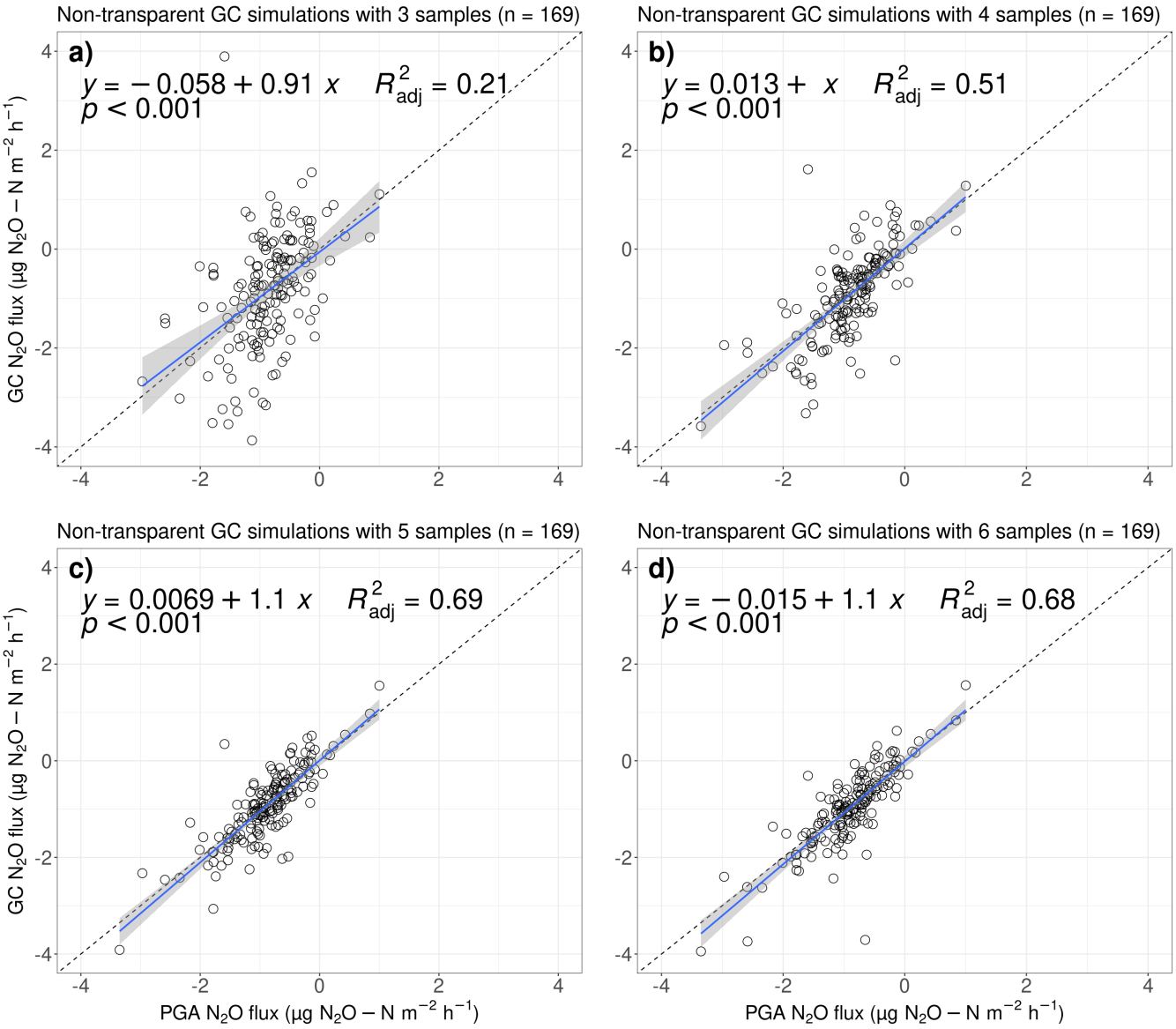

Figure 8. Simulated GC fluxes from opaque measurements with a) 3, b) 4, c) 5, and d) 6 samples compared to flux measurements taken with our PGA for 10 min (n = 338). All fluxes were calculated with the goFlux package; results from "best.Flux" are shown. The blue trend line fits a generalised linear model, with the shaded area representing the 95% confidence interval. The shown equations and R^2_{adj} values follow the $y \sim x$ equation.

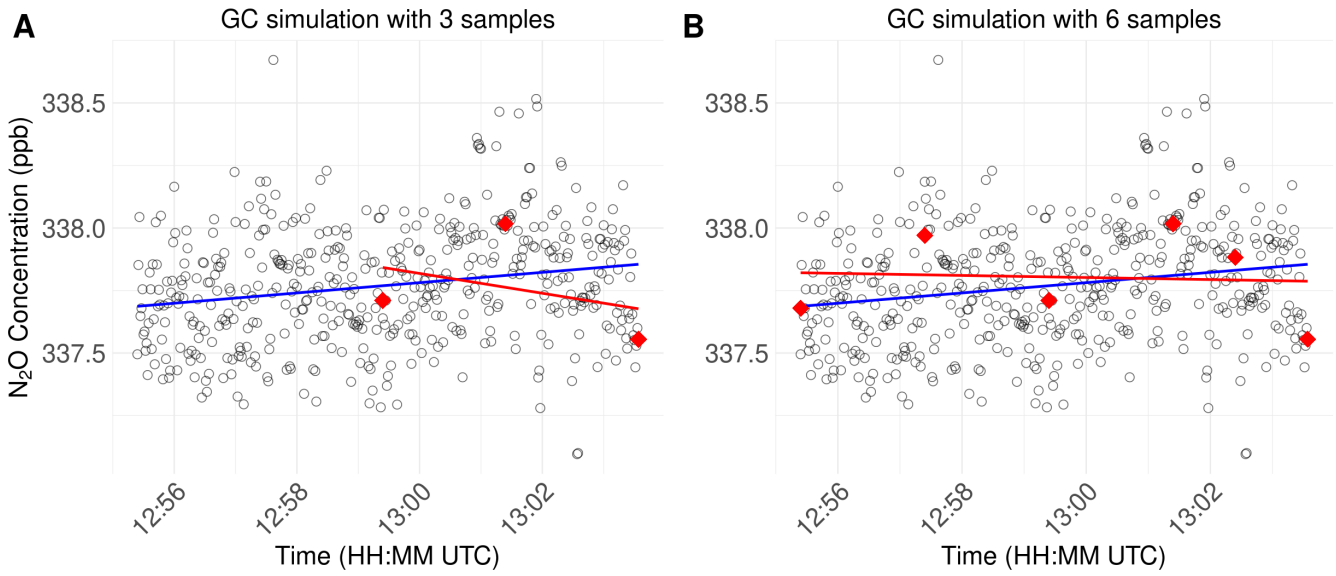

Figure 9. Examples visualising the comparison of regression slopes obtained using 600 data points from the portable gas analyser (blue line) vs 3 (A) or 6 (B) virtual samples mimicking manually defined sample times for subsequent analysis in a gas chromatograph (red line), respectively.

be discarded if only one sample is erroneous. In contrast, using four to six samples yield very comparable results to those obtained with a PGA, depending on the precision of the GC method. However, the small sample size restricts our ability to confidently identify trends in N_2O fluxes. Undetected errors can bias flux estimates due to the high impact of each data point on the regression slope. To compare previous N_2O flux measurements to novel data sets measured with a PGA, it is crucial to investigate differences between these methods. To achieve this, novel instruments have to be tested on their precision, noise, and accuracy, as well as potential interference with water vapour (Grace et al., 2020; Ahmed et al., 2024).

We suggest that measuring N_2O fluxes with fast-responding analysers in nutrient-poor ecosystems should be considered for all future studies. PGAs, for example, have two main advantages over the GC method: they collect a large amount of sample points, and the quality of these can be checked *in situ* during the measurement period. With more samples, there are more data points, which then results in the option to reduce chamber closure times and further reduce artefacts caused by sealing off a part of a soil profile by a closed chamber (Brümmer et al., 2017). If errors happen in the field, *e.g.*, leakage and pressure change (Rochette and Hutchinson, 2015), they are visible in the online interface of the PGA. This real-time *in situ* control of N_2O concentrations allows for direct optimisation in the field and increases the quality of flux measurements (Fiedler et al., 2022). A practical result of that is that measurement periods can be interrupted and repeated in the field at any time, ensuring high quality of the flux measurements, as well as an optimal use of time in the field, particularly since chamber closure times with PGAs are shorter than with GCs. However, PGAs have some drawbacks: weighing 10-20 kg (including batteries), they are heavier than GC vials. Additionally, their power consumption requires regular backups, and factors such as heavy vibrations,

particles, water, and sudden pressure changes can contaminate the laser cell (Fiedler et al., 2022). With good planning and care, it is, however, easily possible to deal with these disadvantages.

4 Conclusions

In our study, we established a manual flux chamber method using a portable gas analyser (PGA) capable of quantifying low N_2O fluxes in nutrient-poor ecosystems and, based on our extensive experience with the system, provide detailed practical suggestions on how to collect high-quality measurements in low-flux ecosystems (see SI). To our knowledge, our study represents the first extensive analysis of N_2O fluxes measured with manual flux chambers in a (very) nutrient-poor, (sub-) Arctic ecosystem. Our laboratory tests confirmed that our PGA (Aeris MIRA Ultra N_2O / CO_2) is well suited for measuring low N_2O fluxes, with low noise, minimal water interference, and negligible signal drift. With our PGA- chamber system, we are able to report very low N_2O flux values with positive and negative signs, indicating both N_2O efflux and uptake. Because PGAs allow for near-continuous monitoring of concentration changes with high precision and low detection limits, we recommend, with a chamber height of 25 cm, chamber closure times of 3-5 min for opaque and >4 min for transparent measurements to minimise the impacts of the ecosystem due to the measurement setup (*e.g.*, changes in temperature and humidity). To strike a balance between detection sensitivity and measurement efficiency, we suggest using a standard 5-minute closure time for all measurements with smaller chambers, which enables us to detect around 70% of fluxes. This allows for most N_2O fluxes to be detected in this setup; however, the sensitivity depends on the effective chamber height.

We further recommend using non-linear models for N_2O flux calculations (HM; (Hutchinson and Mosier, 1981)), with filters to address overestimation at higher flux rates. Novel software packages such as goFlux (Rheault et al., 2024) simplify the integration of both linear and non-linear models, and report flux rates in a reproducible way; such approaches are key to standardising flux calculations across the chamber community. Using non-linear models, as well as standardised and well-documented calculation and quality control, allows to consider the entire time series of measurement periods, and does not require (subjective) expert knowledge to first restrict the datasets to a suitable section, and only afterwards calculate flux estimates. We stress this importance of using all available data points for flux estimates to improve the reproducibility and consistency of N_2O flux estimates.

We recommend using PGAs in future N_2O studies in nutrient-poor ecosystems whenever feasible. PGAs collect more data points (typically about 1 sample / second) and allow for real-time quality control in the field, while GC measurements may be limited by low flux rates and thus fall below the detection limits or lack clear trends. To get the most out of PGAs, it is essential to determine their precision and use a suitable chamber closure time. In that way, most N_2O fluxes can be detected, which is especially important in nutrient-poor ecosystems, where N_2O fluxes are often very low. Future studies using other chamber designs may benefit from re-evaluating chamber closure times and flux calculation methods to find optimum customised setups.

While this study concentrates on the methodological aspects of quantifying N_2O fluxes in a nutrient-poor ecosystem, a follow-up study will investigate the environmental drivers of N_2O fluxes. Because most studies in the (sub-) Arctic have reported N_2O from opaque measurements only, there is a lack of data on how soil N_2O fluxes differ in various light conditions,

especially in Arctic ecosystems (Stewart et al., 2012). Our results demonstrate notable differences between transparent and opaque conditions that require further investigation. This fills an important gap in N_2O studies from the Arctic, where negative fluxes have been observed, but could not be investigated due to measurement accuracy not being high enough (Voigt et al., 2020). Further, this novel finding highlights the need for future research on N_2O fluxes in sub-Arctic ecosystems and other nutrient-poor ecosystems, and their potential response to global warming.

Code availability. The scripts for processing and analysing the data are publicly available at https://git.bgc-jena.mpg.de/ntriches/data-analysis/-/tags/2024-12-12-triches-amtsubmission-n2oadvances under the terms of the GNU General Public License version 3.

Appendix A

Sampling ambient air using Aeris-N_2O analyser, Fig. A1 shows the entire 15 hours long run without removing the first 5 hours (1 Hz), where the water vapour mole fractions were not stable.

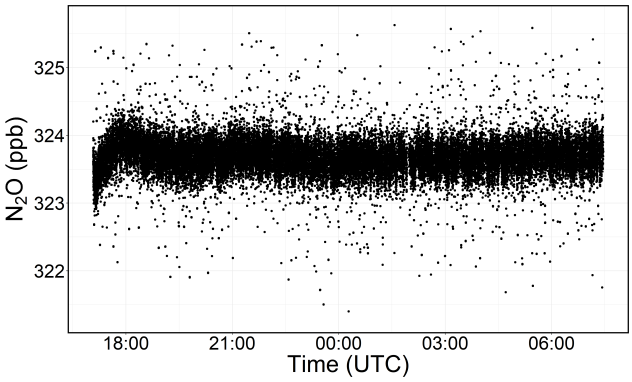

Figure A1. Time series of the N_2O-Analyser of 15 hrs long run.

Changes of H_2O mole fractions during the water interference test (see Fig. A2). Corresponding relative humidity values were noted and the data used for the comparison were designated with red vertical lines.

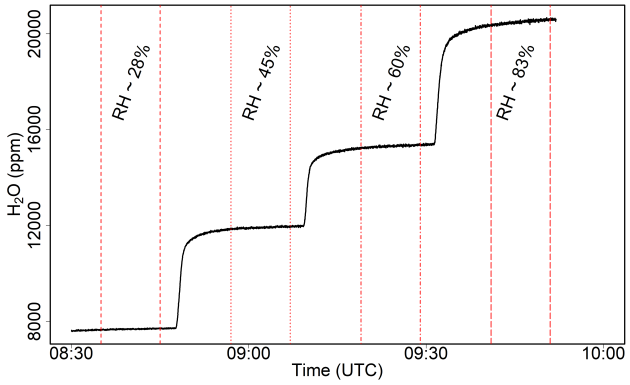

Figure A2. H_2O mole fractions measured by Aeris-N_2O analyser during the water interference test. The corresponding relative humidity (RH) values were given for each step. Red lines demonstrate the data used to assess the water interference at each RH steps.

Author contributions. NYT designed the experiment, collected, and processed the data, and did the laboratory test together with AB. AB further analysed and reported the laboratory data, and created the QGIS figures. NYT and JE developed and implemented the scripts used for data processing, quality checks, analysis, and GC simulations. TV wrote the mathematical explanation of non-linear and linear models. NYT wrote the first draft of the manuscript, and AB, AMV, MEM, MG, MH and TV provided valuable comments that helped improving it. NYT was supervised by MG, MH, TV, AMV, and MEM. MH and MG were responsible for funding acquisition.

Competing interests. The authors declare that they have no conflict of interest.

Acknowledgements. The presented research was supported by the European Research Council (ERC) under the European Union's Horizon 2020 research and innovation programme (grant agreement No 951288, Q-Arctic) and by ICOS-Finland (University of Helsinki).The work of MEM was financed by Research Council of Finland-funded projects Thaw-N (no. 353858) and N-Perm (no. 341348). AMV acknowledges funding catalyzed by the TED Audacious Project (Permafrost Pathways).

The authors thank the 'Field experiments & instrumentation', 'Mechanical and electronics workshops' and 'GasLab' service groups at the Max Planck Institute for Biogeochemistry for their help in designing the chamber system and testing the Aeris-N_2O. We also thank Christina Biasi and Richard Lamprecht who helped with the experiment design and setup. Further thanks to the field assistants Alena Markelova, Antonin Affolder, Mark Schlutow, Mirkka Rovamo, Valentin Kriegel and Wasi Hashmi, as well as the staff from the Abisko Scientific Research Station and Mattias Dalkvist. Many thanks to Karelle Rheault for her continuous help with the goFlux package, and Jesper Christiansen for support in the interpretation of non-linear and linear flux rates. Authors also thank Danilo Custódio and Nicholas J. Eves at MPI-BGC/BSI for their valuable comments and suggestions which helped us improve this manuscript.

References

Ahmed, W., Osborne, E. L., Veluthandath, A. V., and Senthil Murugan, G.: A Rapid and Simplified Approach to Correct Atmospheric Absorptions in Infrared Spectra, Analytical Chemistry, p. acs.analchem.4c03594, https://doi.org/10.1021/acs.analchem.4c03594, 2024.

Allan, D. W.: Should the Classical Variance Be Used As a Basic Measure in Standards Metrology?, IEEE TRANSACTIONS ON INSTRUMENTATION AND MEASUREMENT, 36, 1987.

Anthony, W. H., Hutchinson, G. L., and Livingston, G. P.: Chamber Measurement of Soil-Atmosphere Gas Exchange: Linear vs. Diffusion-Based Flux Models, Soil Science Society of America Journal, 59, 1308–1310, https://doi.org/10.2136/sssaj1995.03615995005900050015x, 1995.

Brümmer, C., Lyshede, B., Lempio, D., Delorme, J.-P., Rüffer, J. J., Fuß, R., Moffat, A. M., Hurkuck, M., Ibrom, A., Ambus, P., Flessa, H., and Kutsch, W. L.: Gas chromatography vs. quantum cascade laser-based N₂O flux measurements using a novel chamber design, Biogeosciences, 14, 1365–1381, https://doi.org/10.5194/bg-14-1365-2017, 2017.

Buchen, C., Roobroeck, D., Augustin, J., Behrendt, U., Boeckx, P., and Ulrich, A.: High N2O Consumption Potential of Weakly Disturbed Fen Mires with Dissimilar Denitrifier Community Structure, Soil Biology and Biochemistry, 130, 63–72, https://doi.org/10.1016/j.soilbio.2018.12.001, 2019.

Callaghan, T. V., Jonasson, C., Thierfelder, T., Yang, Z., Hedenås, H., Johansson, M., Molau, U., Van Bogaert, R., Michelsen, A., Olofsson, J., Gwynn-Jones, D., Bokhorst, S., Phoenix, G., Bjerke, J. W., Tømmervik, H., Christensen, T. R., Hanna, E., Koller, E. K., and Sloan, V. L.: Ecosystem change and stability over multiple decades in the Swedish subarctic: complex processes and multiple drivers, Philosophical Transactions of the Royal Society B: Biological Sciences, 368, 20120 488, https://doi.org/10.1098/rstb.2012.0488, 2013.

Christensen, T. R., Michelsen, A., and Jonasson, S.: Exchange of CH4 and N2O in a subarctic heath soil: effects of inorganic N and P and amino acid addition, Soil Biology and Biochemistry, 31, 637–641, 1999.

Christiansen, J. R., Outhwaite, J., and Smukler, S. M.: Comparison of CO2, CH4 and N2O soil-atmosphere exchange measured in static chambers with cavity ring-down spectroscopy and gas chromatography, Agricultural and Forest Meteorology, 211-212, 48–57, https://doi.org/10.1016/j.agrformet.2015.06.004, 2015.

Clough, T. J., Rochette, P., Thomas, S. M., Pihlatie, M., Christiansen, J. R., and Thorman, R. E.: Global Research Alliance N_2 O chamber methodology guidelines: Design considerations, Journal of Environmental Quality, 49, 1081–1091, https://doi.org/10.1002/jeq2.20117, 2020.

Cowan, N. J., Famulari, D., Levy, P. E., Anderson, M., Bell, M. J., Rees, R. M., Reay, D. S., and Skiba, U. M.: An improved method for measuring soil N_2 O fluxes using a quantum cascade laser with a dynamic chamber, European Journal of Soil Science, 65, 643–652, https://doi.org/10.1111/ejss.12168, 2014.

Davidson, E. A., Savage, K., Verchot, L. V., and Navarro, R.: Minimizing artifacts and biases in chamber-based measurements of soil respiration, Agricultural and Forest Meteorology, 113, 21–37, https://doi.org/10.1016/S0168-1923(02)00100-4, number: 1, 2002.

De Klein, C. A. M., Harvey, M. J., Clough, T. J., Petersen, S. O., Chadwick, D. R., and Venterea, R. T.: Global Research Alliance N_2 O chamber methodology guidelines: Introduction, with health and safety considerations, Journal of Environmental Quality, 49, 1073–1080, https://doi.org/10.1002/jeq2.20131, 2020.

Denmead, O. T.: Approaches to measuring fluxes of methane and nitrous oxide between landscapes and the atmosphere, Plant and Soil, 309, 5–24, https://doi.org/10.1007/s11104-008-9599-z, number: 1-2, 2008.

Elberling, B., Christiansen, H. H., and Hansen, B. U.: High nitrous oxide production from thawing permafrost, Nature Geoscience, 3, 332–335, https://doi.org/10.1038/ngeo803, 2010.

Fiedler, J., Fuß, R., Glatzel, S., Hagemann, U., Huth, V., Jordan, S., Jurasinski, G., Kutzbach, L., Maier, M., Schäfer, K., Weber, T., and Weymann, D.: BEST PRACTICE GUIDELINE: Measurement of carbon dioxide, methane and nitrous oxide fluxes between soil-vegetation-systems and the atmosphere using non-steady state chambers, 2022.

Fleck, D., He, Y., Herman, D., Moseman-valtierra, S., and Jacobson, G. A.: Comparison of a Gas Chromatograph and a Cavity Ringdown Spectrometer for Flux Quantification of Nitrous Oxide, Carbon Dioxide and Methane in Closed Soil Chambers Derek Fleck1, Yonggang He1, Donald Herman2, Serena Moseman-Valtierra3, Gloria Jacobson1 1 Picarro Inc, 3105 Patrick Henry Drive, Santa Clara, CA 95054 2 College of Natural Resource, UC Berkeley, 130 Mulford Hall, University of California, Berkeley, CA, 94720-3114 3 University of Rhode Island, CBLS 489, Kingston, RI 02881, 2013, B11F–0428, https://ui.adsabs.harvard.edu/abs/2013AGUFM.B11F0428F, conference Name: AGU Fall Meeting Abstracts ADS Bibcode: 2013AGUFM.B11F0428F, 2013.

Grace, P. R., Weerden, T. J., Rowlings, D. W., Scheer, C., Brunk, C., Kiese, R., Butterbach-Bahl, K., Rees, R. M., Robertson, G. P., and Skiba, U. M.: Global Research Alliance N $_2$ O chamber methodology guidelines: Considerations for automated flux measurement, Journal of Environmental Quality, 49, 1126–1140, https://doi.org/10.1002/jeq2.20124, number: 5, 2020.

Grogan, P., Michelsen, A., Ambus, P., and Jonasson, S.: Freeze–thaw regime effects on carbon and nitrogen dynamics in sub-arctic heath tundra mesocosms, Soil Biology and Biochemistry, 36, 641–654, https://doi.org/10.1016/j.soilbio.2003.12.007, 2004.

Hensen, A., Skiba, U., and Famulari, D.: Low cost and state of the art methods to measure nitrous oxide emissions, Environmental Research Letters, 8, 025 022, https://doi.org/10.1088/1748-9326/8/2/025022, 2013.

Hutchinson, G. L. and Mosier, A. R.: Improved Soil Cover Method for Field Measurement of Nitrous Oxide Fluxes, SOIL SCI. SOC. AM. J., 45, 6, 1981.

Hübschmann, H.: Handbook of GC-MS: Fundamentals and Applications, Wiley, 1 edn., ISBN 978-3-527-33474-2 978-3-527-67430-5, https://doi.org/10.1002/9783527674305, 2015.

Hüppi, R., Felber, R., Krauss, M., Six, J., Leifeld, J., and Fuß, R.: Restricting the nonlinearity parameter in soil greenhouse gas flux calculation for more reliable flux estimates, PLOS ONE, 13, e0200 876, https://doi.org/10.1371/journal.pone.0200876, publisher: Public Library of Science (PLoS), 2018.

IPCC: Climate Change 2021 – The Physical Science Basis: Working Group I Contribution to the Sixth Assessment Report of the Intergovernmental Panel on Climate Change, Cambridge University Press, 1 edn., ISBN 978-1-009-15789-6, https://doi.org/10.1017/9781009157896, 2023.

Jonasson, C., Sonesson, M., Christensen, T. R., and Callaghan, T. V.: Environmental Monitoring and Research in the Abisko Area—An Overview, AMBIO, 41, 178–186, https://doi.org/10.1007/s13280-012-0301-6, 2012.

Jungkunst, H. F., Meurer, K. H. E., Jurasinski, G., Niehaus, E., and Günther, A.: How to Best Address Spatial and Temporal Variability of Soil-derived Nitrous Oxide and Methane Emissions, Journal of Plant Nutrition and Soil Science, 181, 7–11, https://doi.org/10.1002/jpln.201700607, 2018.

Kroon, P. S., Hensen, A., Van Den Bulk, W. C. M., Jongejan, P. A. C., and Vermeulen, A. T.: The importance of reducing the systematic error due to non-linearity in N2O flux measurements by static chambers, Nutrient Cycling in Agroecosystems, 82, 175–186, https://doi.org/10.1007/s10705-008-9179-x, 2008.

Kutzbach, L., Schneider, J., Sachs, T., Giebels, M., Nykänen, H., Shurpali, N. J., Martikainen, P. J., Alm, J., and Wilmking, M.: CO₂ flux determination by closed-chamber methods can be seriously biased by inappropriate application of linear regression, Biogeosciences, 4, 1005–1025, https://doi.org/10.5194/bg-4-1005-2007, 2007.

Leiber-Sauheitl, K., Fuß, R., Voigt, C., and Freibauer, A.: High CO₂ fluxes from grassland on histic Gleysol along soil carbon and drainage gradients, Biogeosciences, 11, 749–761, https://doi.org/10.5194/bg-11-749-2014, 2014.

Livingston, G. P. and Hutchinson, G. L.: Enclosure-based measurement of trace gas exchange: applications and sources of error, in: Biogenic Trace Gases: Measuring Emissions from Soil and Water (P.A. Matson and R.C. Harriss (eds.)), pp. 14–51, John Wiley & Sons, ISBN 978-1-4443-1381-9, google-Books-ID: WDjpgK7IQAgC, 1995.

Lundin, E., Crill, P., Grudd, H., Holst, J., Kristoffersson, A., Meire, A., Mölder, M., and Rakos, N.: ETC L2 ARCHIVE, Abisko-Stordalen Palsa Bog, 2022-01-01–2024-09-01, https://hdl.handle.net/11676/e22P1IhSEko3C-2eEIZrVMf6, 2024.

Malmer, N., Johansson, T., Olsrud, M., and Christensen, T. R.: Vegetation, climatic changes and net carbon sequestration in a North-Scandinavian subarctic mire over 30 years, Global Change Biology, 11, 1895–1909, https://doi.org/10.1111/j.1365-2486.2005.01042.x, 2005.

Martikainen, P. J., Nykänen, H., Crill, P., and Silvola, J.: Effect of a Lowered Water Table on Nitrous Oxide Fluxes from Northern Peatlands, Nature, 366, 51–53, https://doi.org/10.1038/366051a0, 1993.

Marushchak, M. E., Pitkämäki, A., Koponen, H., Biasi, C., Seppälä, M., and Martikainen, P. J.: Hot spots for nitrous oxide emissions found in different types of permafrost peatlands: NITROUS OXIDE FLUXES FROM PERMAFROST PEATLANDS, Global Change Biology, 17, 2601–2614, https://doi.org/10.1111/j.1365-2486.2011.02442.x, 2011.

Myhre, G., Shindell, D., Bréon, F.-M., Collins, W., Fuglestvedt, J., Huang, J., Koch, D., Lamarque, J.-F., Lee, D., Mendoza, B., Nakajima, T., Robock, A., Stephens, G., Zhang, H., Aamaas, B., Boucher, O., Dalsøren, S. B., Daniel, J. S., Forster, P., Granier, C., Haigh, J., Hodnebrog, , Kaplan, J. O., Marston, G., Nielsen, C. J., O'Neill, B. C., Peters, G. P., Pongratz, J., Ramaswamy, V., Roth, R., Rotstayn, L., Smith, S. J., Stevenson, D., Vernier, J.-P., Wild, O., Young, P., Jacob, D., Ravishankara, A. R., and Shine, K.: Anthropogenic and Natural Radiative Forcing, in: Climate Change 2013: The Physical Science Basis. Contribution of Working Group I to the Fifth Assessment Report of the Intergovernmental Panel on Climate Change [Stocker, T.F., D. Qin, G.-K. Plattner, M. Tignor, S.K. Allen, J. Boschung, A. Nauels, Y. Xia, V. Bex and P.M. Midgley (eds.)], p. 82, Cambridge University Press, Cambridge, United Kingdom and New York, USA, https://www.ipcc.ch/site/assets/uploads/2018/02/WG1AR5_Chapter08_FINAL.pdf, 2013.

Parkin, T. B. and Venterea, R. T.: USDA-ARS GRACEnet project protocols, chapter 3. Chamber-based trace gas flux measurements, Sampling protocols. Beltsville, MD p, pp. 1–39, 2010.

Pavelka, M., Acosta, M., Kiese, R., Altimir, N., Brümmer, C., Crill, P., Darenova, E., Fuß, R., Gielen, B., Graf, A., Klemedtsson, L., Lohila, A., Longdoz, B., Lindroth, A., Nilsson, M., Jiménez, S. M., Merbold, L., Montagnani, L., Peichl, M., Pihlatie, M., Pumpanen, J., Ortiz, P. S., Silvennoinen, H., Skiba, U., Vestin, P., Weslien, P., Janous, D., and Kutsch, W.: Standardisation of chamber technique for CO2, N2O and CH4 fluxes measurements from terrestrial ecosystems, International Agrophysics, 32, 569–587, https://doi.org/10.1515/intag-2017-0045, number: 4, 2018.

Pedersen, A. R., Petersen, S. O., and Schelde, K.: A comprehensive approach to soil-atmosphere trace-gas flux estimation with static chambers, European Journal of Soil Science, 61, 888–902, https://doi.org/10.1111/j.1365-2389.2010.01291.x, 2010.

Pumpanen, J., Kolari, P., Ilvesniemi, H., Minkkinen, K., Vesala, T., Niinistö, S., Lohila, A., Larmola, T., Morero, M., Pihlatie, M., Janssens, I., Yuste, J. C., Grünzweig, J. M., Reth, S., Subke, J.-A., Savage, K., Kutsch, W., Østreng, G., Ziegler, W., Anthoni, P., Lindroth, A.,

and Hari, P.: Comparison of Different Chamber Techniques for Measuring Soil CO2 Efflux, Agricultural and Forest Meteorology, 123, 159–176, https://doi.org/10.1016/j.agrformet.2003.12.001, 2004.

Repo, M. E., Susiluoto, S., Lind, S. E., Jokinen, S., Elsakov, V., Biasi, C., Virtanen, T., and Martikainen, P. J.: Large N2O emissions from cryoturbated peat soil in tundra, Nature Geoscience, 2, 189–192, https://doi.org/10.1038/ngeo434, 2009.

Rheault, K., Christiansen, J. R., and Larsen, K. S.: goFlux: A user-friendly way to calculate GHG fluxesyourself, regardless of user experience, Journal of Open Source Software, 9, 6393, https://doi.org/10.21105/joss.06393, 2024.

Rochette, P. and Eriksen-Hamel, N. S.: Chamber Measurements of Soil Nitrous Oxide Flux: Are Absolute Values Reliable?, Soil Science Society of America Journal, 72, 331–342, https://doi.org/10.2136/sssaj2007.0215, 2008.

Rochette, P. and Hutchinson, G. L.: Measurement of Soil Respiration in Situ: Chamber Techniques, in: Agronomy Monographs, edited by Hatfield, J. and Baker, J., pp. 247–286, American Society of Agronomy, Crop Science Society of America, and Soil Science Society of America, Madison, WI, USA, ISBN 978-0-89118-268-9 978-0-89118-158-3, https://doi.org/10.2134/agronmonogr47.c12, 2015.

Savage, K., Phillips, R., and Davidson, E.: High temporal frequency measurements of greenhouse gas emissions from soils, Biogeosciences, 11, 2709–2720, https://doi.org/10.5194/bg-11-2709-2014, number: 10, 2014.

Schlesinger, W. H.: An Estimate of the Global Sink for Nitrous Oxide in Soils, Global Change Biology, 19, 2929–2931, https://doi.org/10.1111/gcb.12239, 2013.

Siewert, M. B.: High-resolution digital mapping of soil organic carbon in permafrost terrain using machine learning: a case study in a sub-Arctic peatland environment, Biogeosciences, 15, 1663–1682, https://doi.org/10.5194/bg-15-1663-2018, 2018.

Sjögersten, S., Ledger, M., Siewert, M., De La Barreda-Bautista, B., Sowter, A., Gee, D., Foody, G., and Boyd, D. S.: Optical and radar Earth observation data for upscaling methane emissions linked to permafrost degradation in sub-Arctic peatlands in northern Sweden, Biogeosciences, 20, 4221–4239, https://doi.org/10.5194/bg-20-4221-2023, 2023.

Stewart, K. J., Brummell, M. E., Farrell, R. E., and Siciliano, S. D.: N2O flux from plant-soil systems in polar deserts switch between sources and sinks under different light conditions, Soil Biology and Biochemistry, 48, 69–77, https://doi.org/10.1016/j.soilbio.2012.01.016, 2012.

Subke, J.-A., Kutzbach, L., and Risk, D.: Soil Chamber Measurements, in: Springer Handbook of Atmospheric Measurements, edited by Foken, T., pp. 1603–1624, Springer International Publishing, Cham, ISBN 978-3-030-52170-7 978-3-030-52171-4, https://doi.org/10.1007/978-3-030-52171-4_60, series Title: Springer Handbooks, 2021.

Thoning, K., Dlugokencky, E., Lan, X., and NOAA Global Monitoring Laboratory: Trends in globally-averaged CH4, N2O, and SF6, https://doi.org/10.15138/P8XG-AA10, 2022.

Varner, R. K., Crill, P. M., Frolking, S., McCalley, C. K., Burke, S. A., Chanton, J. P., Holmes, M. E., Isogenie Project Coordinators, Saleska, S., and Palace, M. W.: Permafrost thaw driven changes in hydrology and vegetation cover increase trace gas emissions and climate forcing in Stordalen Mire from 1970 to 2014, Philosophical Transactions of the Royal Society A: Mathematical, Physical and Engineering Sciences, 380, 20210 022, https://doi.org/10.1098/rsta.2021.0022, 2022.

Venterea, R. T. and Baker, J. M.: Effects of Soil Physical Nonuniformity on Chamber-Based Gas Flux Estimates, Soil Science Society of America Journal, 72, 1410–1417, https://doi.org/10.2136/sssaj2008.0019, 2008.

Virkkala, A.-M., Niittynen, P., Kemppinen, J., Marushchak, M. E., Voigt, C., Hensgens, G., Kerttula, J., Happonen, K., Tyystjärvi, V., Biasi, C., Hultman, J., Rinne, J., and Luoto, M.: High-resolution spatial patterns and drivers of terrestrial ecosystem carbon dioxide, methane, and nitrous oxide fluxes in the tundra, Biogeosciences, 21, 335–355, https://doi.org/10.5194/bg-21-335-2024, 2024.

Voigt, C., Marushchak, M. E., Abbott, B. W., Biasi, C., Elberling, B., Siciliano, S. D., Sonnentag, O., Stewart, K. J., Yang, Y., and Martikainen, P. J.: Nitrous oxide emissions from permafrost-affected soils, Nature Reviews Earth & Environment, 1, 420–434, https://doi.org/10.1038/s43017-020-0063-9, 2020.

Widén, B. and Lindroth, A.: A Calibration System for Soil Carbon Dioxide-Efflux Measurement Chambers: Description and Application, Soil Science Society of America Journal, 67, 327–334, https://doi.org/10.2136/sssaj2003.3270, 2003.

Łakomiec, P., Holst, J., Friborg, T., Crill, P., Rakos, N., Kljun, N., Olsson, P.-O., Eklundh, L., Persson, A., and Rinne, J.: Field-scale CH₄ emission at a subarctic mire with heterogeneous permafrost thaw status, Biogeosciences, 18, 5811–5830, https://doi.org/10.5194/bg-18-5811-2021, 2021.